Numerical study of high impedance T-match antennas for terahertz photomixers

JUUL, Lars, MIKULICS, Martin, PEREIRA, Mauro <http://orcid.org/0000-0002-2276-2095> and MARSO, Michel

Published version

JUUL, Lars, MIKULICS, Martin, PEREIRA, Mauro and MARSO, Michel (2014). Numerical study of high impedance T-match antennas for terahertz photomixers. Optical and Quantum Electronics, 47 (4), 913-922.

Noname manuscript No.
(will be inserted by the editor)

Numerical Study of High Impedance T-match Antennas for Terahertz Photomixers

Lars Juul · Martin Mikulics · Mauro F. Pereira · Michel Marso

Received: date / Accepted: date

Abstract This paper outlines an efficient numerical method to design terahertz photomixers. The simulations are benchmarked using measured power levels from results published in the literature. Next, the method is applied to two new photomixer designs based on the high impedance T-match antenna with bias supply DC-blocking structures for either a uniplanar layout or a multilayer structure for improved device reliability. Manufacturability is favoured by avoiding the use of airbridges, substrate thinning or under-etching. The estimated output power of the improved design is 9.0 μW, which is an improvement of 3 times over the reference photomixer.

Keywords Photoconductor Impedance · Terahertz Photomixer · Numerical Simulation · T-match Antenna

1 Introduction

Commercial applications of terahertz technology are inhibited by a lack of compact, inexpensive tunable sources with a large dynamic range for continuous wave (CW) spectroscopy and imaging purposes. THz Quantum cascade lasers (QCLs) (Köhler et al, 2002) already deliver over 1 W of pulsed power (Li et al, 2014). However they require cryocooling, e.g. for 3.4 THz emission this record laser has a maximum operating temperature of 123 K. Furthermore, they are extremely

L. Juul, M. Marso
Université Du Luxembourg, Research Unit for Engineering Science, L-1359 Luxembourg, Luxembourg
E-mail: lars.juul@uni.lu; michel.marso@uni.lu

M. Mikulics
Peter Grünberg Institute (PGI-9), Forschungscentrum Jülich, D-52425 Jülich, Germany
E-mail: M.Mikulics@fz-juelich.de

M. Pereira
Sheffield Hallam University, Materials and Engineering Research Institute, Sheffield S1 1WB, United Kingdom
E-mail: M.Pereira@shu.ac.uk

expensive and their predicitive design requires advanced mathematical physics approaches, such as Nonequilibrium Greens Functions Theories (Schmielau and Pereira, 2009c,a,b; Wacker et al, 2013). Photomixing technology is far from delivering this level or power but is far less expensive to design and fabricate and has the further advantage of room temperature operation.

Furthermore resonant tunneling diode oscillators (Asada and Suzuki, 2013) have made significant progress towards the production of a high power source in the terahertz region, but the simplicity of heterodyne photomixers in concept and manufacturing continue to make them a compelling option for room temperature CW sources.

Several attempts to increase the photomixer output power through high impedance antenna designs have been made (Duffy et al, 2001; Han et al, 2010; Juul et al, 2012). This work describes the design of two photomixer high impedance antenna structures, based on the T-match antenna by (Kraus and Sturgeon, 1940) with two options for DC-blocking structures.

2 Outline of the Numerical Method

One of the technology specific challenges for the heterodyne photomixer is the low terahertz current delivered to the antenna. The terahertz current, i_{thz}, for a given optical beat frequency, ω, can found using the AC-responsivity relation given by (Mikulics, 2004):

$$i_{thz} = P_{in} V_b \frac{\eta e \lambda \mu \tau_c}{hcl^2} (1 + \omega^2 \tau_c^2)^{-\frac{1}{2}} \tag{1}$$

where λ is the optical source wavelength, c is the speed of light, h is Planck's constant, l is the electrode distance, P_{in} is the total optical input power, V_b is the bias voltage, η is the quantum efficiency of the optical absorption process, e is the elementary charge, τ_c is the average carrier lifetime, and μ is the photocarrier mobility in the ultrafast semiconductor. The radiated output power from an antenna is given by (Balanis, 2005), p. 82:

$$P_{rad} = i^2 r_{rad} \tag{2}$$

where i is the rms current into the antenna terminals and r_{rad} is the radiation resistance, which is the part of the input resistance actually giving rise to radiation.

We now use the known dimensions and the experimental results for the D1-D3 dipole photomixers with identical photoconductors from (Duffy et al, 2001) to obtain an estimate of the photocurrent. The peak output power of the D1-D3 designs have been measured experimentally as $3\,\mu$W at 0.85 THz, $2\,\mu$W at 1.05 THz and $0.5\,\mu$W at 1.6 THz. We performed a numerical simulation of the D1-D3 radiation resistances using CST Microwave Studio® 2013. The frequency domain solver was chosen for the task along with a tetrahedral mesh with adaptive mesh refinement due to its suitability for inclusion of smaller features in an otherwise electrically large structure. The 1 μm LT GaAs layer is not modelled in the simulation, as the low temperature growth and subsequent annealing only gives rise to a limited change ($\Delta n \simeq 0.25$) in refractive index (Dankowski et al, 1994). Additionally, the poorly conducting Ti adhesion layer has not been modelled, and only the Au thickness has been accounted for in the simulations. The Au conductor loss

has been modelled by manually entering the data points for frequency dependent surface resistance, obtained using a Drude model in accordance with the recommendation from (Lucyszyn, 2003). The substrate is assumed lossless, due to the annealing of the LT GaAs layer and an otherwise highly resistive GaAs base layer (Blakemore, 1982). Port parasitics were modelled with 0.75 fF excess capacitance and the excitation was performed with an infinite impedance current port. When driving the D1 structure with a port current of 145 μA, we obtain a radiated power of approximately 3 μW at 0.85 THz.

Figure 1 shows the calculated AC photocurrent i_{thz} using equation (1) at $\omega_{ref} = 2\pi \cdot 0.85$ THz, where the average photocarrier lifetime is $\tau_c = 300$ fs (Duffy et al, 2001), mobility value is $\mu = 0.01$ m^{2}V^{-1}s^{-1} (Brown, 2003), an optical source wavelength of $\lambda = 850$ nm, and an electrode gap of $l = 0.8$ μm (Duffy et al, 2001) for an optical power range from 0 to 35 mW and a bias voltage range from 0 to 15 V. The $i_{thz,ref} = 145$ μA predicted by CST Microwave Studio® can be obtained theoretically if an optical input power of 20 mW and a bias voltage of 10 V are applied.

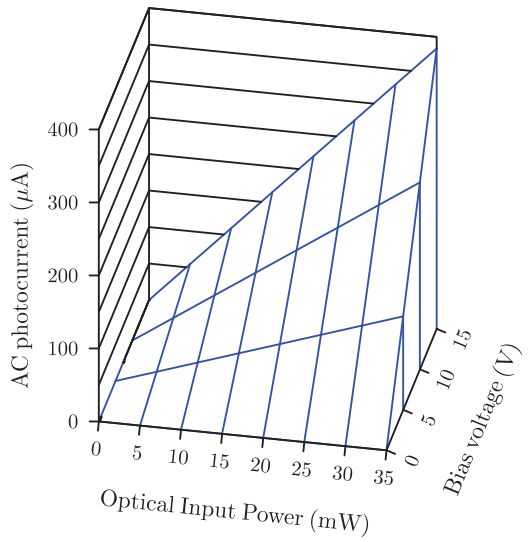

Fig. 1 Calculated AC photocurrent of an LT GaAs photoconductor at 0.85 THz with $\mu = 0.01$ m^{2}V^{-1}s^{-1}, $\tau_c = 300$ fs, $\eta = 0.43$, and $l = 0.8\,\mu$m using 850 nm optical sources.

We can now calculate the radiated output power P_{rad} for any given frequency, ω, using equation (2):

$$P_{rad} = r_{rad}\, i_{thz}^2 = r_{rad} \frac{i_{0,ref}^2}{1 + \omega^2 \tau_c^2} \tag{3}$$

where $i_{0,ref}$ is the normalised photocurrent, without the influence of the bandwidth limiting average carrier lifetime, τ_c: $i_{0,ref} = i_{thz,ref} \sqrt{1 + \omega_{ref}^2 \tau_c^2}$. Using τ_c = 300 fs, ω_{ref} = 0.85 THz and $i_{thz,ref}$ = 145 μA we get $i_{0,ref}$ = 274 μA. The

radiation resistance, r_{rad}, for D1 to D3 is found by dividing the radiated power, $P_{rad,sim}$ with the square value of the port current, $i_{port,sim}$.

This allows us to directly calculate the predicted power levels of the simulated structures using the values from (Duffy et al, 2001) and equation (3). Figure 2 shows the simulation results for the photomixers D1-D3 by applying our method. Data points for actual measurements have been superimposed and show good coherence between experiment and simulation.

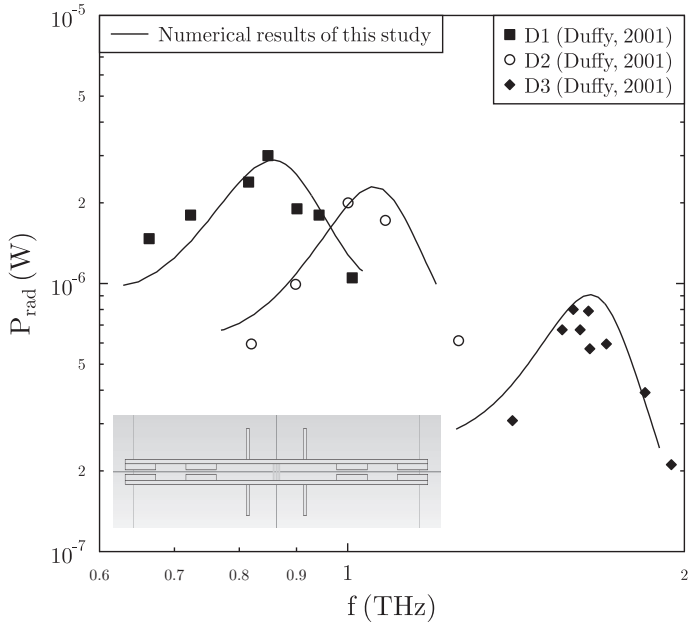

Fig. 2 Numerical results for the output power P_{rad} of the dual dipoles D1-D3 from (Duffy et al, 2001) though application of our simulation method with experimentally measured power levels superimposed. Inset: D1 photomixer simulation model.

3 Numerical Results and Discussion

Next, we propose our two new solutions, Design I and Design II, based on the T-match antenna by (Kraus and Sturgeon, 1940) each with two options, a uniplanar metal-semiconductor-metal (MSM) structure or a multilayer stack, for the DC-blocking structures.

The T-match antenna is a classical antenna structure which features a higher input resistance, as a result of multiple simultaneous radiating elements, requiring less current to achieve a similar output power compared to that of an equivalent dipole antenna. The antenna consists of a long dipole element with a shorter driving element dipole tapped at the $\lambda/4$ and $3\lambda/4$ points of the larger full wave dipole. According to (Balanis, 2005), p. 532, the input impedance of a lossless wire

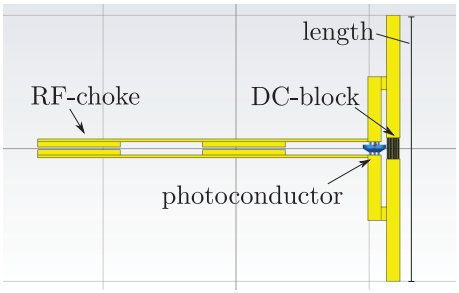

Fig. 3 Design I: Based on a T-match antenna with a uniplanar MSM DC-blocking capacitance.

version of the T-match antenna is approximately:

$$Z_{in} \approx (1 + \alpha^2) Z_a \tag{4}$$

where α is the current division factor between the two dipoles (α is unity in case of equal antenna cross sections) and Z_a is the input impedance of the structure without the T-match connection.

Design I is a photomixer based on the T-match antenna with a 0.3 μm thick Au planar conductor on a thin Ti adhesive layer on a GaAs substrate with a 1 μm LT GaAs layer (Figure 3). The antenna dimensions are designed for full wave operation and a DC-blocking MSM finger structure is inserted into the long dipole element, to prevent the photomixer bias supply from encountering a short circuit. A $\lambda/4$ RF-choke is added to the design to prevent terahertz current from leaking into the bias supply.

Parameter sweeping results suggests that a conductor width of 5 μm is a suitable dimension for the structure, allowing for enough MSM area for the DC-block to achieve terahertz AC-conductance. Furthermore, the width allows for an incorporation of a 5 μm x 5 μm photoconductor area without discontinuities. The optimum size for the gap between the dipole elements is approximately 2 μm. The choke segment length is 30 μm. In order to provide an adequate coupling, the DC-block finger width and spacing must be on the order of 200 nm. The length of the MSM structure is 8 μm in the direction parallel to the dipoles.

Figure 4 shows the Design I radiation resistance for antenna lengths from 96 μm to 108 μm, reaching a consistent 300 Ω around 0.85 THz, implying a $P_{rad,est} = (150\,\mu\text{A})^2 \cdot 300\,\Omega = 6.8\,\mu\text{W}$.

Design II is developed as follows: The T-match antenna input impedance can be further increased, if an additional long dipole element is placed next to the driving short dipole element. This can be achieved by mirroring the structure consisting of the long dipole element including the DC-block, the tapping connections, and the RF-choke (Figure 5).

The radiation resistance for Design II with an antenna length from 96 μm to 111 μm with uniplanar MSM DC-blocks (Figure 6) is subject to a roll-off beyond 0.8 THz, with an estimated output power at 0.85 THz of 6.1 μW. The roll-off can be explained by the changed charge distribution on the centre dipole as the proximity effect will have an influence on the charge distribution on the long dipole elements, and consequently in the charge distribution on the MSM, where the current is concentrated near the inner edge along the gap between the dipoles.

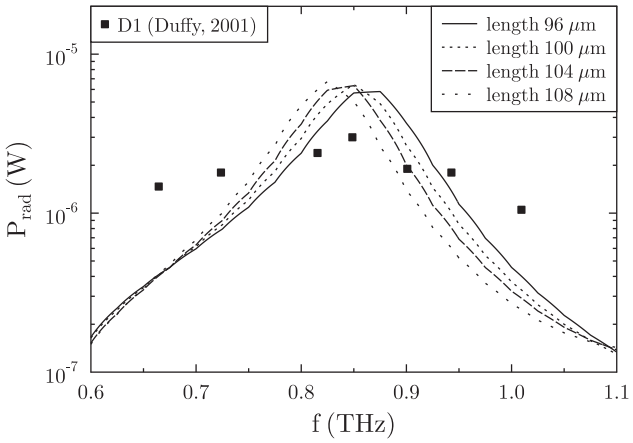

Fig. 4 Numerical results for the radiation resistance r_{rad} of Design I with an MSM DC-blocking capacitance.

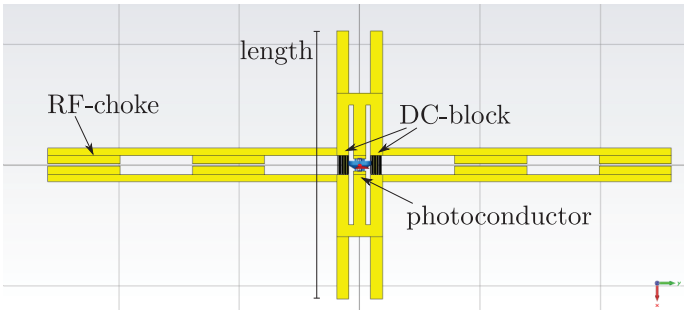

Fig. 5 Design II: An extension of the T-match antenna with an additional long dipole element. Choke and DC-blocks are kept symmetrical

Adding an additional long dipole element next to the driving dipole element will invariably change the current density of the latter. A changed charge distribution across the MSM will affect its reactive properties and thus its efficacy as a DC-block.

The uniplanar MSM-finger structure used for the DC-blocking requires sophisticated patterning methods in manufacturing and is also sensitive to high current densities increasing the risk of device failure over time. A more reliable capacitive structure with larger metal cross sections could consist of overlapping conductors separated by a layer of 0.1 μm silicon nitride. The lower layer conductors are separated by a 1 μm gap and the whole structure occupies the exact same area (5 μm x 8 μm) as the uniplanar MSM (Figure 7).

The performance of Design I with a multilayer DC-block remains largely unchanged (Figure 8) compared to the MSM-version (Figure 4). The radiated ouput

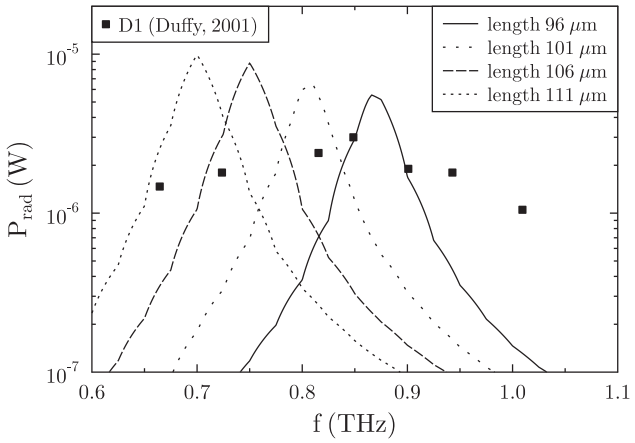

Fig. 6 Numerical results for the radiation resistance r_{rad} of Design II with an MSM DC-blocking capacitance.

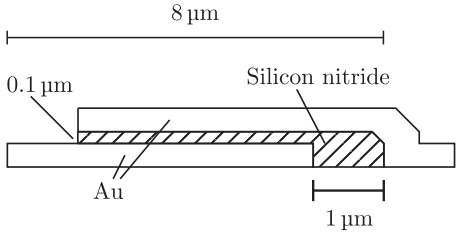

Fig. 7 Cross section of a multilayer DC-blocking structure. The metal layers are separated by a thin nitride layer. The structure occupies the same 5 μm x 8 μm surface area as the MSM DC-block

power stays at 6.8 μW. This suggests that the MSM DC-block works as intended for the Design I layout.

Design II with a multilayer DC-block shows a greatly improved radiation resistance of 400 Ω at 0.85 THz (Figure 9), resulting in a radiated power of $P_{rad,est} = 9.0\,\mu$W, which is an improvement of 3 times over D1 from (Duffy et al, 2001). The multilayer DC-block supplies a large enough reactance, such that it becomes invariant towards the current distribution on the centre dipole.

4 Conclusion

This work has presented a way of estimating photomixer output power levels by applying our simulation methodology to determine the radiation resistance of a known photomixer with measured output power results in order to find the

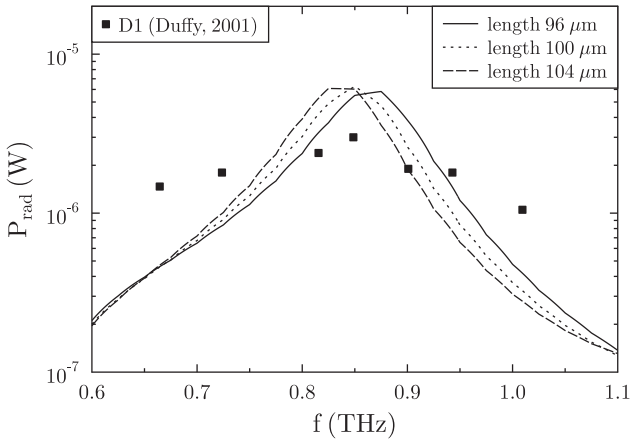

Fig. 8 Numerical results for the radiation resistance r_{rad} of Design I with a multilayer DC-block structure.

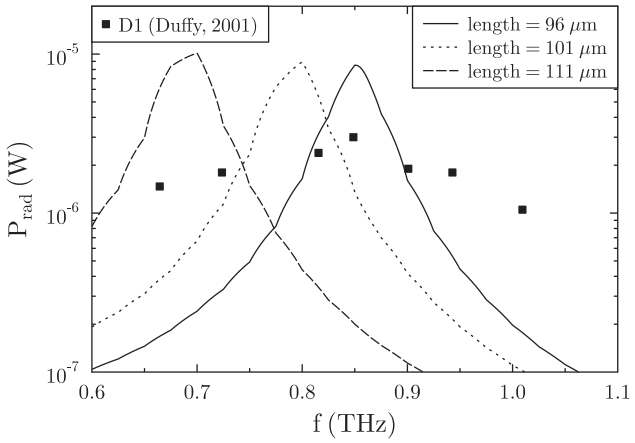

Fig. 9 Numerical results for the radiation resistance r_{rad} of Design II with a multilayer DC-blocking capacitance.

photoconductor THz ac-current. This allows for output power prediction for new photomixer structures simulated with similar features in terms of photoconductor layout, substrate dielectric constant, and conductor material.

We have delivered two new implementations of the classical T-match antenna, adapted to a planar layout with bias supply DC-blocking. Design I features the classical two conductor approach, and Design II is a novel version of the T-match structure consisting of three conductors. The estimated output power of the Design

I photomixer becomes 6.8 μW at 0.85 THz, compared to 6.1 μW for the Design II version.

The MSM configuration of the DC-block is thought to be the reason for the unexpected lower performance, which is confirmed by replacing it with a multilayer DC-blocking structure. The performance of Design I with a multilayer DC-block is unchanged at 6.8 μW, whereas the Design II photomixer with the multilayer DC-block has an estimated output power of 9.0 μW This is an improvement of 3 times over the baseline of 3.0 μW at 0.85 THz from (Duffy et al, 2001). An additional advantage of using multilayer DC-blocks for Design I or II is the improvement in device lifetime as a result of avoiding the current sensitive, narrow 200 nm conductors required for the MSM.

The designs avoid the use of airbridges, under-etching, and substrate thinning for manufacturability purposes and can be directly incorporated for a range of technologies, including LT GaAs, LT InGaAs and N:GaAs, where a high impedance antenna is needed for THz sources with a weak current drive.

Acknowledgments

The authors wish to thank MPNS COST ACTION MP1204 - TERA-MIR Radiation: Materials, Generation, Detection and Applications for support as well as CST A/G, Darmstadt, Germany for providing the university license for CST Microwave Studio 2013.

References

Asada M, Suzuki S (2013) Compact THz oscillators with resonant tunneling diodes and application to high-capacity wireless communications

Brown ER (2003) THz generation by photomixing in ultrafast photoconductors. International Journal of High Speed Electronics and Systems, 13(2):497–545

Balanis CA (2005) Antenna Theory, 3rd edn. John Wiley & Sons

Blakemore JS (1982) Semiconducting and other major properties of gallium arsenide. Journal of Applied Physics , vol.53, no.10, R123

Dankowski SU, Kiesel P, Knupfer B, Kneissl M, Dohler GH, Keil UD, Dykaar DR, Kopf RF (1994) Annealing induced refractive index and absorption changes of lowtemperature grown GaAs. Applied Physics Letters , vol.65, no.25, pp.3269–3271

Duffy SM, Verghese S, McIntosh KA, Jackson A, Gossard AC, Matsuura S (2001) Accurate modelling of dual dipole and slot elements used with photomixers for coherent terahertz output power. IEEE Transactions on Microwave Theory and Techniques 49(6):1032–1038

Han K, Nguyen T, Park I, Han H (2010) Terahertz yagi-uda antenna for high input resistance. Journal of Infrared, Millimeter and Terahertz Waves 31:441–454

Juul L, Mikulics M, Marso M (2012) Improving output power of terahertz heterodyne photomixer by impedance matching. In: 2012 Ninth International Conference on Advanced Semiconductor Devices & Microsystems (ASDAM)

Köhler R, Tredicucci A, Beltram F, Beere H, Linfield E, Davies A, Ritchie D, Iotti R, Rossi F (2002) Terahertz semiconductor-heterostructure laser. Nature 417(6885):156–159

Kraus JD, Sturgeon SS (1940) The t-matched antenna. QST 9:24–25

Li L, Chen L, Zhu J, Freeman J, Dean P, Valavanis A, Davies A, Linfield E (2014) Terahertz quantum cascade lasers with >1 W output powers. Electronics Letters 50(4):309–311

Lucyszyn S (2003) Accurate CAD modelling of metal conduction losses at terahertz frequencies. Electron Devices for Microwave and Optoelectronic Applications, 2003. EDMO 2003. The 11th IEEE International Symposium on , pp.180–185

Mikulics M (2004) Preparation and optimization of low-temperature-grown GaAs photomixers. PhD thesis, Rheinisch-Westfälische Technische Hochschule Aachen

Schmielau T, Pereira M (2009a) Impact of momentum dependent matrix elements on scattering effects in quantum cascade lasers. Physica Status Solidi (B) Basic Research 246(2):329–331

Schmielau T, Pereira M (2009b) Momentum dependent scattering matrix elements in quantum cascade laser transport. Microelectronics Journal 40(4-5):869–871

Schmielau T, Pereira M (2009c) Nonequilibrium many body theory for quantum transport in terahertz quantum cascade lasers. Applied Physics Letters 95(23)

Wacker A, Lindskog M, Winge D (2013) Nonequilibrium Green's function model for simulation of quantum cascade laser devices under operating conditions. IEEE Journal on Selected Topics in Quantum Electronics 19(5)